

## COMMUNICATION

# Reversible Unfolding of $\beta$ -Sheets in Membranes: A Calorimetric Study

William C. Wimley<sup>1\*</sup> and Stephen H. White<sup>2</sup>

<sup>1</sup>Department of Biochemistry  
SL43, Tulane University Health  
Sciences Center, New Orleans  
LA 70112-2699, USA

<sup>2</sup>Department of Physiology and  
Biophysics and the Program in  
Macromolecular Structure  
University of California at  
Irvine, Irvine, CA 92697-4560  
USA

The hexapeptide acetyl-Trp-Leu<sub>5</sub> (AcWL<sub>5</sub>) has the remarkable ability to assemble reversibly and spontaneously into  $\beta$ -sheets on lipid membranes as a result of monomer partitioning followed by cooperative assembly. This system provides a unique opportunity to study the thermodynamics of protein folding in membranes, which we have done using isothermal titration calorimetry (ITC) and differential scanning calorimetry (DSC). The results, which may represent the first example of reversible thermal unfolding of peptides in membranes, help to define the contribution of hydrogen bonding to the extreme thermal stability of membrane proteins. ITC revealed that the enthalpy change for partitioning of monomeric, unstructured AcWL<sub>5</sub> from water into membranes was zero within experimental error over the temperature range of 5 °C to 75 °C. DSC showed that the  $\beta$ -sheet aggregates underwent a reversible, endothermic, and very asymmetric thermal transition with a concentration-dependent transition temperature ( $T_m$ ) in the range of 60 °C to 80 °C. A numerical model of nucleation and growth-dependent assembly of oligomeric  $\beta$ -sheets, proposed earlier to describe  $\beta$ -sheet formation in membranes, recreated remarkably well the unusual shape and concentration-dependence of the transition peaks. The enthalpy for thermal unfolding of AcWL<sub>5</sub>  $\beta$ -sheets in the membrane was found to be about  $8(\pm 1)$  kcal mol<sup>-1</sup>, or about  $1.3(\pm 0.2)$  kcal mol<sup>-1</sup> per residue.

© 2004 Elsevier Ltd. All rights reserved.

**Keywords:** membrane proteins; protein folding;  $\beta$ -barrel; membrane-induced folding; nucleation

\*Corresponding author

## Introduction

The thermodynamic driving forces for membrane protein (MP) folding and assembly are not fully understood quantitatively. One reason for this is that reversible thermal unfolding transitions of membrane-buried secondary structure elements cannot be observed,<sup>1</sup> because of the high thermodynamic cost of breaking H-bonds in the non-polar membrane interior. The free energy cost can exceed 80–100 kcal mol<sup>-1</sup> for a 20 amino acid (AA) transmembrane (TM)  $\alpha$ -helix.<sup>2</sup> The few available calorimetric studies of MPs detect only the thermal

unfolding of extra-membrane domains and the rearrangement of membrane-spanning segments,<sup>1</sup> and even these transitions are mostly irreversible. The goal of the work described here was to use a peptide model system for which reversible unfolding transitions in the membrane are experimentally accessible (Figure 1) in order to obtain quantitative information about the forces that stabilize membrane proteins.

Beginning with the seminal calorimetric measurements of Privalov and colleagues 30 years ago,<sup>3–7</sup> the thermodynamics of unfolding single-domain soluble proteins have been described well, both experimentally and theoretically.<sup>8–10</sup> Soluble proteins are only marginally stable with a net free energy of folding,  $\Delta G_{\text{fold}}$ , ranging from  $-5$  to  $-15$  kcal mol<sup>-1</sup>, corresponding to transition midpoint temperatures ( $T_m$ ) in the range of 50–90 °C. The small  $\Delta G_{\text{fold}}$  value for soluble proteins in the aqueous phase apparently arises from strong

Abbreviations used: AcWL<sub>5</sub>, acetyl-Trp-Leu<sub>5</sub>; ITC, isothermal titration calorimetry; DSC, differential scanning calorimetry; TM, transmembrane; POPC, palmitoyl-oleoyl-phosphocholine.

E-mail address of the corresponding author:  
wwimley@tubane.edu

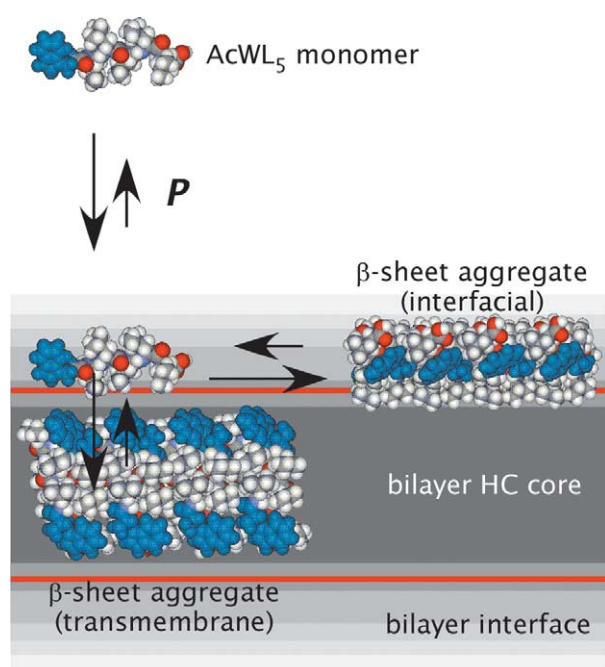


**Figure 1.** Schematic outline of the assembly of AcWL<sub>5</sub>  $\beta$ -sheets in membranes in two possible configurations. In aqueous solution of phospholipid vesicles there is an equilibrium between monomeric random-coils in water and in the membrane interface, described by a partition coefficient  $P$ . If the concentration in the membrane is increased above a threshold of about 0.001 peptides per lipid, AcWL<sub>5</sub> assembles cooperatively and reversibly into antiparallel oligomeric  $\beta$ -sheets.<sup>41,42</sup> Two possible aggregate configurations are shown schematically, interfacial and transmembrane.<sup>42</sup> The correct configuration is not known, but in either case the Trp and C-terminal carboxyl groups must be in the interface. Trp residues are colored blue. The schematic image of the interfacial aggregates is a view along the axes of the  $\beta$ -strands, which are aligned normal to the plane of the Figure.

thermodynamic compensation between the stabilizing hydrophobic effect and destabilizing polar group/peptide bond dehydration, described in detail by Yang *et al.*<sup>11</sup> The free energy balance for MPs is problematic, because of the difficulty of unfolding them inside membranes.

The literature contains only a few accounts of the thermal denaturation of membrane proteins. In one of the earliest references, Jackson & Sturtevant<sup>12</sup> reported the irreversible denaturation of the membrane protein bacteriorhodopsin at about 100 °C in its native membrane. Bacteriorhodopsin has since been studied by other laboratories as well, and these studies invariably find that bacteriorhodopsin in membranes undergoes an irreversible structural transition in the temperature range 90 °C to 100 °C. FTIR spectroscopy<sup>13,14</sup> showed that the protein retained much of its  $\alpha$ -helical structure even above the transition temperature. This is in full agreement with structural studies of the thermal unfolding of cytochrome *c* oxidase, for example. The multiple

transitions of cytochrome *c* oxidase were interpreted as resulting from unfolding of extrinsic domains and an irreversible structural rearrangement of membrane-spanning segments, which did not unfold.<sup>15–17</sup> Similar results have been reported for bovine rhodopsin,<sup>18</sup> the GLUT1 glucose transporter,<sup>19</sup> a Ca<sup>2+</sup> ATPase,<sup>16,17,20</sup> and a mechanosensitive channel of *Escherichia coli*.<sup>21</sup> Like bacteriorhodopsin, most of these membrane proteins have high-temperature thermal transitions that have scan-rate-dependent calorimetric properties. This means that the transitions were irreversible, because the high temperature state converted irreversibly to an additional state. This thermally induced, inactive state could have resulted from aggregated protein in the membrane or from a state with non-native topology. As further evidence of incomplete unfolding of these membrane proteins, their calorimetric enthalpies for the thermal transitions have a mean value of about 0.35 ( $\pm 0.05$ ) kcal mol<sup>-1</sup> per residue. This is about half of the value of that measured for soluble proteins,<sup>22</sup> and less than one-third the value we report here for AcWL<sub>5</sub> unfolding in membranes (see below). The image that emerges from this literature is that the thermal denaturation of membrane proteins is an irreversible and kinetically controlled process, rather than an equilibrium process, and that it does not involve the unfolding of the membrane-spanning segments. The membrane-spanning segments are thus very stable toward unfolding. Because of this, published calorimetric studies of membrane protein folding are of little utility in understanding the thermodynamic driving forces for membrane protein folding.

Direct experimental measurements of the energetics of peptide folding and unfolding in membranes to date is limited to our studies of AcWL<sub>5</sub> folding<sup>23,24</sup> and a few studies of interfacial folding of amphipathic  $\alpha$ -helices and their diastereomeric analogs.<sup>25–27</sup> Membrane partitioning and secondary structure formation of polypeptides in the membrane are coupled through the cost of partitioning the peptide bond.<sup>28</sup> Specifically, the partitioning of an open peptide bond from water into the bilayer interface is unfavorable<sup>28</sup> by at least 1.2 kcal mol<sup>-1</sup>. The reduction of that unfavorable interaction in the membrane through the formation of intramolecular H-bonds is the primary driving force for the formation of secondary structure.<sup>23</sup> Thus, relative to folding in an aqueous environment, a peptide partitioned into a membrane will be much more likely to have secondary structure.<sup>2</sup> Based on several model peptide studies, the net free energy of secondary structure formation for peptides in membranes, including the contribution of hydrogen bonding, configurational entropy, and bilayer effects,<sup>29</sup> is in the range of  $-0.15$  to  $-0.7$  kcal mol<sup>-1</sup> per residue.<sup>24–27,30</sup> We have estimated that the assembly of AcWL<sub>5</sub>  $\beta$ -sheets in membranes is driven by a favorable folding free energy of 0.4–0.6 kcal mol<sup>-1</sup> per residue.<sup>24</sup>

Considering that a TM  $\beta$ -barrel contains a minimum of 80 residues<sup>31</sup> and a TM  $\alpha$ -helix is about 20 residues long,<sup>32</sup> the net H-bond driving force for structure formation in membranes can be very large, consistent with the extreme thermal stability of membrane-spanning proteins.<sup>1</sup>

AcWL<sub>5</sub> is a well-characterized hexapeptide that folds cooperatively in membranes into large oligomeric  $\beta$ -sheets.<sup>23,24</sup> Oligomers assemble in membranes *via* a three-step process of monomer partitioning,  $\beta$ -sheet nucleation, and  $\beta$ -sheet growth.<sup>24</sup> This reversible (equilibrium) folding process, illustrated schematically in Figure 1, produces membrane  $\beta$ -sheets that are estimated to contain 10–20 peptides each.<sup>24</sup> The reversible unfolding of AcWL<sub>5</sub> is clearly revealed by circular dichroism (CD) spectroscopy measurements. Plots of molar ellipticity at 199 nm *versus* temperature revealed a characteristic secondary-structure melting curve with an inflection at about 60 °C and transition half-width of about 20 °C, consistent with the cooperative melting of 50 or more residues (see Figure 6 of Wimley *et al.*<sup>24</sup>). However, the melting was not the result of a simple two-state transition, because the collection of CD spectra gathered at different temperatures did not have an isodichroic point. In the work described here, we present calorimetric studies of folding/unfolding reactions of AcWL<sub>5</sub>  $\beta$ -sheets that provide further insights into the melting transition in membranes and hence the energetics of MP stability.

### Thermodynamics of membrane partitioning of AcWL<sub>5</sub>

The folding–unfolding equilibria of AcWL<sub>5</sub>, outlined in Figure 1, include the thermally induced  $\beta$ -sheet-to-coil transition on (or possibly in) the

membrane and the membrane-to-aqueous phase partitioning of the unfolded peptides.<sup>24</sup> The latter transition makes this a particularly convenient experimental system, because the AcWL<sub>5</sub> peptides that unfold in the membrane can also partition into the aqueous phase, and thereby remove the penalty associated with the partitioning of open H-bonds into the membrane. This couples  $\beta$ -sheet unfolding to a shift of peptide molecules from the membrane to the aqueous phase.<sup>24</sup> In contrast, the high hydrophobicity of full-length MPs prevents their partitioning into the aqueous phase during thermal unfolding. In our experiments, we have studied both the partitioning and unfolding of AcWL<sub>5</sub> by calorimetry. Isothermal titration calorimetry (ITC) was used to characterize the partitioning step and differential scanning calorimetry (DSC) to characterize the thermal unfolding step. Together, they provide a complete image of the thermodynamics of  $\beta$ -sheet unfolding in membranes.

The ITC measurements, designed to measure the enthalpy of water-to-membrane partitioning ( $\Delta H_m$ ) of unfolded AcWL<sub>5</sub>, were made under conditions in which  $\beta$ -sheets do not form:<sup>24</sup> high lipid concentration (100 mM lipid) and low peptide concentration ( $\leq 10 \mu\text{M}$  AcWL<sub>5</sub>). Under these conditions,<sup>24</sup> the peptide is a monomeric, interfacially bound, random-coil with a free-energy of transfer  $\Delta G_m = -5.2 \text{ kcal mol}^{-1}$ . We also measured the  $\Delta H_m$  value for AcWL<sub>4</sub>, which has nearly identical<sup>33</sup> membrane interactions but does not form  $\beta$ -sheets at any concentration, because it has a much higher water solubility. ITC results for the partitioning of monomeric random-coils of both peptides into POPC bilayers are shown in Table 1. Within experimental error, the net enthalpy of partitioning of AcWL<sub>5</sub> was zero across the entire temperature range, which implies a small or zero heat capacity change ( $\Delta C_p$ ) for partitioning as well. This was

**Table 1.** Titration calorimetry results for peptide partitioning into POPC vesicles

Peptide <sup>a</sup>	Concentration (saturated solution) ( $\mu\text{M}$ )	Heat per injection $\pm$ s.e.m. <sup>b</sup> ( $\mu\text{cal}$ )	$\Delta H$ ( $\text{kcal mol}^{-1}$ ) <sup>c</sup>
AcWL <sub>5</sub>	30	$+0.4 \pm 0.7$	$-0.9 \pm 1.5$
AcWL <sub>4</sub>	1100	$0.0 \pm 1.5$	$0.0 \pm 0.1$

<sup>a</sup> Isothermal titration calorimetry (ITC) was done in a Microcal vpITC titration calorimeter. Saturated aqueous solutions of AcWL<sub>5</sub> and AcWL<sub>4</sub> were titrated into 100 mM POPC vesicles made by extrusion.<sup>49</sup> Under these conditions the peptides partition into the vesicles as monomeric random-coils<sup>24</sup> (see Figure 1). The buffer used in all experiments was 10 mM Hepes (pH 7.0), 50 mM KCl, 3 mM NaN<sub>3</sub>, 1 mM EDTA. We included AcWL<sub>4</sub> in this experiment because its membrane interactions are very similar to AcWL<sub>5</sub> under these conditions, but its maximum aqueous concentration is much higher, allowing for a more precise determination of enthalpy. Also, at pH 7, AcWL<sub>4</sub> does not form  $\beta$ -sheets in membranes at any experimentally accessible concentration.

<sup>b</sup> Injection volumes were 15  $\mu\text{l}$ . For each sample, eight consecutive injections were made, and heats of injection were determined by integration. Temperatures used were 5, 25, 50, and 80 °C for AcWL<sub>5</sub> and 25 and 50 °C for AcWL<sub>4</sub>. The heat of injection was the average heat measured for injecting peptide solution into 100 mM POPC minus the heat for injecting peptide into buffer. Neither peptide gave a statistically significant excess heat of injection at any temperature, therefore the values given are the average from all temperatures. Under these conditions of high lipid concentration, both peptides partition into vesicles as monomeric random-coils with about 92% of AcWL<sub>5</sub> and 86% of AcWL<sub>4</sub> partitioning into the membranes. Creating a solution of 100 mM of POPC vesicles is a slow process because of the viscosity of the solution. But beyond the standard procedures, the only additional requirement is patience.

<sup>c</sup> Estimated range of possible enthalpy change ( $\Delta H$ ) for the water bilayer partitioning of each peptide. Values are based on the measured heats of injection and their uncertainties, injection volume, and peptide concentration. The uncertainty in  $\Delta H$  for AcWL<sub>5</sub> is larger than for AcWL<sub>4</sub> because its maximum concentration in a saturated solution is much lower. The mode of interaction of the two peptides under these conditions is nearly identical.<sup>33</sup>

surprising because the hydrophobic effect with characteristic negative heat capacity is generally the main driving force for the partitioning of hydrophobic peptides into membranes. The experimental uncertainty for AcWL<sub>5</sub>, due to its low solubility, was large enough that small, but significant, values of  $\Delta H_m$  and  $\Delta C_p$  could not be excluded. However, measurements performed using the more soluble AcWL<sub>4</sub> peptide also yielded a  $\Delta H_m$  value that was zero within  $\pm 0.1$  kcal mol<sup>-1</sup> at both 25 °C and 50 °C. This observation gives us confidence that the contribution of  $\Delta H_m$  to the thermodynamics of AcWL<sub>5</sub> unfolding in membranes is small.

In order to gain insights into the negligible enthalpy and heat capacity, we examined several other peptides and model compounds. Using exactly the same lipid and buffer system as in this work, we measured  $\Delta H_m$  for the peptides AcWLWLL and AcWLGLL and found values of  $-0.54(\pm 0.2)$  and  $-0.2(\pm 0.1)$  kcal mol<sup>-1</sup>, respectively, at 25 °C with associated heat capacity changes of  $-41$  and  $-18$  cal mol<sup>-1</sup> K<sup>-1</sup> (unpublished observations). In contrast, the 13-residue antimicrobial peptide indolicidin<sup>34</sup> was found to partition exothermically at 25 °C with a  $\Delta H_m$  a value of  $+3.3(\pm 0.5)$  kcal mol<sup>-1</sup> at 25 °C and  $\Delta C_p$  value of  $-330$  cal mol<sup>-1</sup> K<sup>-1</sup>. The bee venom peptide melittin had a  $\Delta H_m$  value of  $+4.0$  kcal mol<sup>-1</sup> at 25 °C with a  $\Delta C_p$  value of  $-300$  cal mol<sup>-1</sup> K<sup>-1</sup> in the same system (unpublished observations). We have also measured  $\Delta H_m$  by ITC for the side-chain analogs of tryptophan (unpublished observations). For *N*-methyl indole and 3-methyl indole,<sup>35</sup> we found values of  $-2.2(\pm 0.2)$  and  $-1.5(\pm 0.2)$  kcal mol<sup>-1</sup>, respectively, with corresponding  $\Delta C_p$  values of  $-17$  and  $-29$  cal mol<sup>-1</sup> K<sup>-1</sup>. If AcWL<sub>4</sub> and AcWL<sub>5</sub> make an exothermic enthalpy contribution to  $\Delta H_m$  due to their tryptophan residues, then there must also be an endothermic contribution from other sources. We speculate that the unfavorable partitioning of the open backbone of these random-coil peptides into the bilayers may be strongly endothermic, possibly due to strong electrostatic interactions with bilayer surfaces.<sup>26</sup> But the interpretation of these and other data in the literature<sup>26,27,30</sup> is further complicated by the induction of structure that accompanies partitioning.<sup>27,30</sup> One can only say at this point that a wide range of partitioning enthalpies and heat capacity changes are possible for peptides interacting with phosphatidylcholine membranes, because of the composite nature of peptide-bilayer interactions<sup>2,36</sup> and the many different competing interactions that contribute.

### Thermodynamics of AcWL<sub>5</sub> folding in membranes

Unlike the ITC measurements, the DSC experiments were done under conditions<sup>24</sup> that promote cooperative assembly of AcWL<sub>5</sub> into multimeric  $\beta$ -sheets: low lipid concentration (2 mM POPC) and

high AcWL<sub>5</sub> concentration (greater than 50  $\mu$ M). We found earlier<sup>24</sup> that the transfer free energy  $\Delta G_{mA}$  of monomer to  $\beta$ -sheet aggregate was  $-3.70$  kcal mol<sup>-1</sup>, and that  $\beta$ -sheet formation was thermally reversible. Upon heating, the membrane-bound  $\beta$ -sheets underwent a cooperative  $\beta$ -sheet-to-coil transition centered at about 65 °C. The peptide was monomeric and unstructured above the transition temperature, and some of the bound peptide partitioned back into the aqueous phase. The DSC experiment was thus expected to measure the energetics of  $\beta$ -sheet unfolding in membranes, and subsequent partitioning of unfolded peptides back into the aqueous phase. Because the  $\Delta H_m$  value for AcWL<sub>5</sub> is zero (Table 1), the enthalpy measured by DSC should therefore represent mainly unfolding of the  $\beta$ -sheets in membranes,  $\Delta H_{mA}$ .

Examples of raw excess heat capacity curves for POPC vesicles and POPC vesicles containing AcWL<sub>5</sub>  $\beta$ -sheets are shown in Figure 2. Except for a small negative shift in the *y*-axis position of the curve, the vesicle-only trace is identical to the water *versus* water instrumental background. This is consistent with the expectation that no thermal transitions occur in POPC over the temperature range<sup>37</sup> of 5 °C to 95 °C. In the vesicles+peptide scan, there is an asymmetric, endothermic transition that occurs over the temperature range of 40 °C to 80 °C. This corresponds exactly to the sheet-to-coil transition observed with CD spectroscopy.<sup>24</sup>

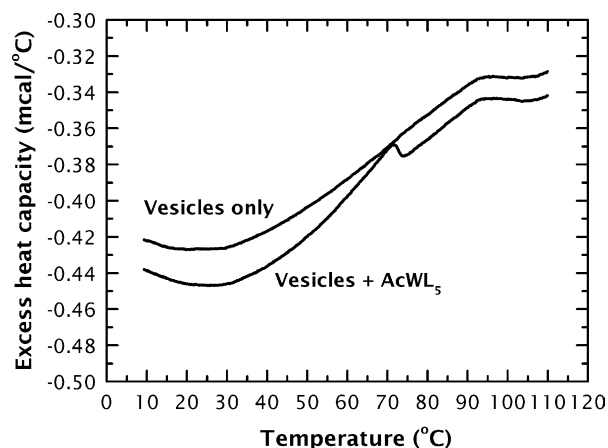


**Figure 2.** Raw differential scanning calorimetry (DSC) data for 2 mM POPC large unilamellar vesicles and for 2 mM POPC vesicles + 79  $\mu$ M AcWL<sub>5</sub>. DSC was done in a Microcal VpDSC calorimeter loaded with buffer in the reference cell. The sample cell contained buffer and lipid, or buffer, lipid and peptide. The scan rate was 60° per minute and the sample cell volume was 0.5185 ml. When the sample cell contained buffer only, the curves were parallel to the buffer + lipid samples. Peptide-containing samples showed an asymmetric, endothermic transition over the range of 40 °C to 80 °C. For all samples, repeated calorimetric scans after the initial scan were nearly identical, demonstrating that the transition is fully reversible. The almost indistinguishable second and third scans of this sample of POPC with AcWL<sub>5</sub> are shown here.

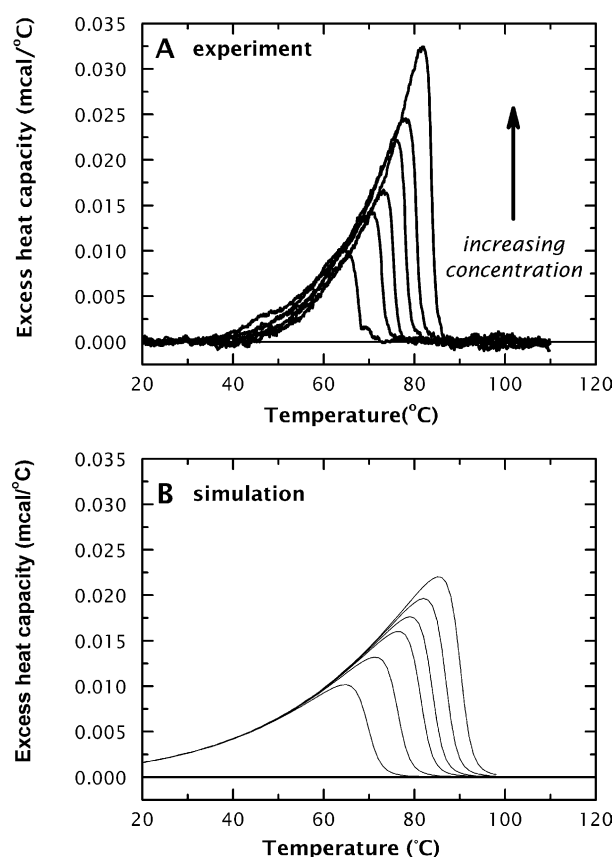


**Figure 3.** Experimental and simulated excess heat capacity peaks for various concentrations of AcWL<sub>5</sub> in 2 mM POPC vesicles. (A) Experimental excess heat capacity measurement. Baselines were estimated using the lipid-only samples that were subtracted from the raw DSC data. Actual peptide concentrations were determined by HPLC<sup>50</sup> after the calorimetry scans. They were 60, 79, 103, 108, 115, and 137  $\mu$ M AcWL<sub>5</sub>. The lipid concentration was 2 mM POPC vesicles. (B) Simulated excess heat capacity curves generated with the nucleation and growth model<sup>24</sup> for AcWL<sub>5</sub> assembly in bilayers. The actual experimental concentrations were used in the simulations. The simulation recreates the unusual shape and concentration-dependence of the unfolding transition in this system.

In Figure 3(A), the baseline-subtracted transition curves are plotted for samples of 2 mM POPC vesicles containing between 60 and 140  $\mu$ M AcWL<sub>5</sub>. Linear baselines were drawn by extrapolation from the regions before and after the transition. We could not detect evidence of a significant shift in baseline heat capacity during the transition. We estimate that we should have been able to measure a baseline heat capacity difference if it were equal to or larger than 0.005  $\text{mcal } ^\circ\text{C}^{-1}$ , which is equivalent to about 100  $\text{cal mol}^{-1} \text{K}^{-1}$  or about 15  $\text{cal mol}^{-1} \text{K}^{-1}$  per residue for 100  $\mu$ M AcWL<sub>5</sub> in the 0.519 ml sample cell. For comparison, a single buried leucine residue in a soluble protein is expected to contribute a heat capacity change of approximately 50  $\text{cal mol}^{-1} \text{K}^{-1}$  upon unfolding.<sup>38</sup> In the ITC experiments (above),

we estimated that the heat capacity change for the water-to-membrane partitioning was smaller than 20  $\text{cal mol}^{-1} \text{K}^{-1}$ . Assuming, then, no baseline heat capacity change, we estimate that the enthalpy of unfolding to be no smaller than 1.3 ( $\pm 0.2$ )  $\text{kcal mol}^{-1}$  per residue (below).

### Numerical modeling of $\beta$ -sheet assembly from AcWL<sub>5</sub>

The asymmetric shape of the DSC transition curves is quite unusual for protein or peptide transitions. As shown in Figure 3(A), these peaks have broad and overlapping leading (i.e. low-temperature) edges, and have very steep high-temperature edges that shift to higher temperatures with higher peptides concentrations. Can the unusual characteristics of these curves be explained with the nucleation-growth model that we have used<sup>24</sup> to explain the assembly of AcWL<sub>5</sub>  $\beta$ -sheets in membranes? To answer this question, we used the model and our previous iterative computational approach to simulate the calorimetry experiment. Briefly, we used the equation<sup>24</sup> for total concentration  $C_T$  of peptide on the membrane:

$$C_T = C_m \left[ 1 - \sigma + \frac{\sigma}{(1 - sC_m)^2} \right] \quad (1)$$

where  $C_m$  is the membrane monomer concentration calculated from the infinite-dilution monomer partition coefficient  $K_x$  (7500) and the equilibrium peptide concentration in water ( $C_w$ ) using  $C_m = K_x C_w / W$ , where  $W$  is the concentration of water (55.3 M). The parameters  $\sigma$  and  $s$  are the nucleation and growth parameters, respectively.<sup>39</sup> For each temperature, the molar concentrations of soluble monomeric peptide ( $C_w$ ), the mole-fraction concentration of bound monomeric peptide ( $C_m$ ), and the mole-fraction concentration of peptide bound as multimeric  $\beta$ -sheets ( $C_{\text{sheet}} = C_T - C_m$ ) were determined from the equations above using values of  $\sigma$  and  $s$  calculated from  $x = \exp(-\Delta G_x / RT)$  and  $\Delta G_x = \Delta H_x - T\Delta S_x$  where  $x = \sigma$  or  $s$ . For simulations using the experimental lipid and peptide concentrations, we found a good empirical match with the experimental data when  $\Delta H_{mA}$  was set to  $-10 \text{ kcal mol}^{-1}$  and  $\Delta G_\sigma$  and  $\Delta G_s$  were set to  $+1.8$  and  $-4.2 \text{ kcal mol}^{-1}$ , respectively. These values are somewhat different from those obtained from partitioning measurements, but are acceptably close given the exquisite sensitivity of the system.<sup>24</sup>

The excess heat capacity curves in the simulation were calculated by numerical integration using:

$$\Delta C_p^{\text{excess}} = \frac{dC_{\text{sheet}}}{dT} (\Delta H_{\text{fold}} LV_{\text{cell}}) \quad (2)$$

where  $C_{\text{sheet}}$  is the mole fraction concentration,  $L$  is the molar lipid concentration (2 mM), and  $V_{\text{cell}}$  is the volume of the calorimeter cell (0.5185 ml). Notice in the simulated curves that all the characteristics of the experimental curves are recreated,

including the unusual shape, asymmetry, concentration-dependence,  $T_m$  values, and the magnitude of  $\Delta C_p^{\text{excess}}$ . We conclude that the very unusual shapes of the calorimetric transitions in AcWL<sub>5</sub>  $\beta$ -sheets in membranes are well accounted for by the nucleation and growth model of AcWL<sub>5</sub> assembly into  $\beta$ -sheets in POPC bilayers.

### Enthalpy of unfolding of AcWL<sub>5</sub> in membranes

The goal of our work was to use the experimentally accessible reversible unfolding transitions of the AcWL<sub>5</sub> system (Figure 1) to obtain quantitative information about the high thermal stability of membrane proteins. Because  $\beta$ -sheets of AcWL<sub>5</sub> in membranes contain 10–20 peptides each,<sup>24</sup> or roughly 100 amino acids, they are comparable in size to small, single-domain proteins. At the same time, because the peptides are water-soluble and only six residues long, it is possible to unfold them thermally in order to study their structural transitions. We show in Figure 4 the concentration-dependence of  $\Delta H_{mA}$  and  $T_m$  for AcWL<sub>5</sub>  $\beta$ -sheet unfolding in membranes. Due in part to increased fractional peptide binding,<sup>33</sup> both values increase with peptide concentration, approaching  $T_m = 80^\circ\text{C}$  and  $\Delta H_{mA} = 7 \text{ kcal mol}^{-1}$  at the highest concentrations of AcWL<sub>5</sub> studied. Based on our earlier work,<sup>24</sup> we estimate that the fractional binding at the highest and lowest peptide concentrations used, 80–90% and 65–80% were bound, respectively. Because the binding/assembly process is extremely cooperative, it is not possible to predict fractional binding more precisely. Dividing the observed enthalpy of unfolding, which increases from 5 to

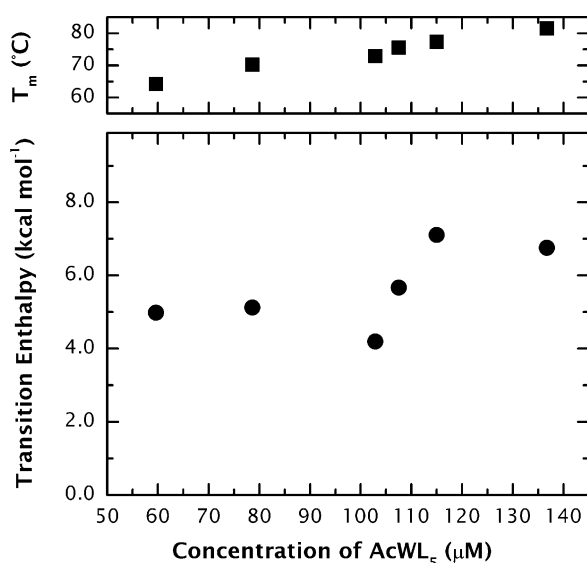


**Figure 4.** Transition enthalpies and  $T_m$  values for the DSC scans shown in Figure 3(A). Uncertainties in the position of the low temperature edge of the broad transition is estimated to contribute an uncertainty in transition enthalpy of about  $\pm 0.5 \text{ kcal mol}^{-1}$  in  $\Delta H$ . The  $T_m$  values are for the maximum in the excess heat capacity curves shown in Figure 3(A).

$7 \text{ kcal mol}^{-1}$  over the range of peptide concentrations studied (Figure 4), by our highest (most conservative) estimates of fractional binding, we obtain a value for the enthalpy of unfolding of no less than  $8(\pm 1) \text{ kcal mol}^{-1}$  of peptide, or about  $1.3(\pm 0.2) \text{ kcal mol}^{-1}$  per residue.

In order to test the reasonableness of this estimate, we examined the thermal unfolding of AcWL<sub>6</sub> in membranes. AcWL<sub>6</sub>, containing a single additional Leu residue, folds into  $\beta$ -sheets in membranes that are very similar to AcWL<sub>5</sub>  $\beta$ -sheets.<sup>24</sup> If each additional hydrogen bond contributes up to  $1.3 \text{ kcal mol}^{-1}$  to stability as our calorimetry results suggest, then AcWL<sub>6</sub>  $\beta$ -sheets will be significantly more stable than those assembled from AcWL<sub>5</sub>. We have reported previously that AcWL<sub>6</sub>  $\beta$ -sheets did not appear to unfold at any experimentally accessible temperature (up to  $100^\circ\text{C}$ ) when examined with CD spectroscopy.<sup>24</sup> DSC measurements performed in conjunction with our measurements for AcWL<sub>5</sub> revealed no evidence of unfolding transitions at any temperature up to  $100^\circ\text{C}$ , confirming the extreme stability of AcWL<sub>6</sub> membrane  $\beta$ -sheets. The excess heat capacity trace for AcWL<sub>6</sub> in POPC (not shown) was essentially identical to the POPC-only trace shown in Figure 2. These results strengthen the idea that hydrogen bonding makes very large net contributions to membrane protein stability.

In order to verify further that our DSC observations for AcWL<sub>6</sub> are reasonable, we performed numerical simulations like those in Figure 3. Simulations were run at the lowest measured concentration of  $\sim 50 \mu\text{M}$  peptide in  $2 \text{ mM}$  lipid using the parameters from the simulation of AcWL<sub>5</sub>. We found that a net increase in the nucleation and growth free energies ( $\Delta G_s$  and  $\Delta G_g$ ; equation (1)) of  $0.5 \text{ kcal mol}^{-1}$  or greater, coupled with the known increase in water-to-membrane partitioning of AcWL<sub>6</sub><sup>33</sup> is sufficient to increase the  $T_m$  value to well over  $100^\circ\text{C}$ . This supports our conclusion from the AcWL<sub>5</sub> data that each hydrogen bond that forms in a membrane environment makes a substantial net contribution to the stability of membrane proteins.

Because  $\Delta H_m$  is zero (Table 1), the enthalpy measured for AcWL<sub>5</sub> unfolding is derived from the unfolding steps in the membrane environment. In contrast, Seelig and colleagues<sup>26,27</sup> have studied the formation of interfacial  $\alpha$ -helices and reported  $\Delta H_{mA}$  of about  $0.7 \text{ kcal mol}^{-1}$  per residue. How do these numbers compare to the enthalpy of unfolding of soluble proteins and peptides in water? As discussed extensively by Yang *et al.*,<sup>11</sup> the per-residue enthalpy accompanying soluble protein unfolding is generally in the range of  $-0.1$  to  $0.6 \text{ kcal mol}^{-1}$ . Scholtz *et al.*,<sup>40</sup> however, found that the per residue enthalpy of unfolding of a 50-residue polyalanine helix to be  $1.3 \text{ kcal mol}^{-1}$ . The difference arises, according to Yang *et al.*,<sup>11</sup> from the electrostatic cost of dehydrating the secondary structure elements when they assemble to form a protein's tertiary structure. That is, there is an

unfavorable enthalpy of dehydration that works against the favorable enthalpy of H-bond formation. What are the consequences of applying this reasoning to the unfolding of our  $\beta$ -sheet aggregates on or in membranes? To begin to address that question, structural information about the membrane aggregates is required.

The three-dimensional structure and topology of the  $\beta$ -sheet aggregates is uncertain, but the available evidence does not rule out the possibility that they may form membrane-spanning structures (Figure 1). Polarized attenuated total reflectance FTIR spectroscopy showed that the interstrand hydrogen bonds are parallel to the membrane surface,<sup>41</sup> consistent with either an interfacial orientation parallel to the membrane surface or transmembrane orientations normal to the bilayer surface (Figure 1). Fluorescence experiments<sup>41,42</sup> are unambiguous in placing the tryptophan residues of the peptide  $\beta$ -sheets in the interfacial region, partially exposed to the aqueous phase. Furthermore, the  $pK_a$  value of 5.7 for the carboxyl termini of the  $\beta$ -sheets change very little (W.C.W, unpublished observations) compared to interfacially bound, random-coil monomers,<sup>43</sup> consistent with an interfacial location of the carboxyl groups. However, in a family of related peptides of the form AcWLLXLL, it was found that only the members with the most non-polar X-residue side-chains assembled readily into multimeric  $\beta$ -sheets. All other side-chains, even those hydrophobic enough to partition strongly into bilayer interfaces, were monomeric random-coils at all concentrations.<sup>42</sup> This acute sensitivity of secondary structure to the polarity of the side-chain at the X-position suggested a mid-bilayer (hydrocarbon core) location for the central residues of the hexapeptide  $\beta$ -sheets, because of the energetic cost of placing a polar moiety in the hydrocarbon core.<sup>42,43</sup> A transmembrane topology would place the carboxy termini and the Trp residues of the  $\beta$ -sheet at the bilayer interfaces, which is consistent with the known interfacial localization of aromatic residues<sup>44</sup> in  $\beta$ -barrel membrane proteins.<sup>45</sup> The transmembrane separation of the Trp residues would be  $\sim 20$  Å, which is rather smaller than the 30 Å thickness<sup>46</sup> of the bilayer hydrocarbon core. Nevertheless, it corresponds closely to the average transmembrane distance between the aromatics of  $\beta$ -barrel membrane proteins<sup>45</sup> and the tryptophan residues of gramicidin dimers.<sup>47,48</sup>

The membrane environment complicates any interpretation of  $\Delta H_{mA}$  because the peptides are in a membrane environment. Changes in lipid–lipid and lipid–protein interactions must surely contribute, but just how is not clear. It may not be surprising then that our value of  $\Delta H_{mA} = 1.3$  kcal mol<sup>-1</sup> per residue for a membrane environment is virtually identical to the enthalpic cost of breaking H-bonds in the unfolding of polyalanine helices in water determined by Scholtz *et al.*<sup>40</sup> This may mean that the  $\beta$ -sheet aggregates are located on the membrane surface with high water exposure. If,

on the other hand, the aggregates have a transmembrane configuration, then the observed value likely arises from a more favorable contribution from H-bonding in the membrane coupled with a very unfavorable enthalpic cost of dehydrating the aggregates upon membrane insertion. In this case, our value of  $\Delta H_{mA}$  represents a lower limit on the enthalpic cost of breaking H-bonds in the non-polar environment of the bilayer hydrocarbon core. Yang *et al.*<sup>11</sup> estimate that the polar group enthalpy favoring the unfolded state of soluble proteins is in the range of  $-0.4$  to  $-1.4$  kcal mol<sup>-1</sup> per residue, suggesting that for buried aggregates the enthalpy for breaking H-bonds in the hydrocarbon core is no smaller than 1.7 to 2.7 kcal mol<sup>-1</sup> per residue.

---

## Acknowledgements

This work was supported by grants GM-46823 (to S.H.W) and GM-60000 (to W.C.W) from the National Institute of General Medical Sciences.

## References

1. Haltia, T. & Freire, E. (1995). Forces and factors that contribute to the structural stability of membrane proteins. *Biochim. Biophys. Acta*, **1241**, 295–322.
2. White, S. H. & Wimley, W. C. (1999). Membrane protein folding and stability: physical principles. *Annu. Rev. Biophys. Biomol. Struct.* **28**, 319–365.
3. Atanasov, B. P., Privalov, P. L. & Khechinashvili, N. N. (1972). Calorimetric investigations on heat denaturation of cyanmetmyoglobin. *Mol. Biol.* **6**, 26–32.
4. Privalov, P. L., Khechinashvili, N. N. & Atanasov, B. P. (1971). Thermodynamic analysis of thermal transitions in globular proteins. I. Calorimetric study of chymotrypsinogen, ribonuclease and myoglobin. *Biopolymers*, **10**, 1865–1890.
5. Privalov, P. L. & Khechinashvili, N. N. (1971). Calorimetric investigation of thermal denaturation of chymotrypsinogen. *Mol. Biol.* **5**, 573–579.
6. Privalov, P. L. & Tiktopulo, E. I. (1970). Thermal conformational transformation of tropocollagen. I. Calorimetric study. *Biopolymers*, **9**, 127–139.
7. Privalov, P. L. & Khechinashvili, N. N. (1974). A thermodynamic approach to the problem of stabilization of globular protein structure: a calorimetric study. *J. Mol. Biol.* **86**, 665–684.
8. Privalov, P. L. & Gill, S. J. (1988). Stability of protein structure and hydrophobic interaction. *Advan. Protein Chem.* **39**, 191–234.
9. Privalov, P. L. & Makhatadze, G. I. (1993). Contribution of hydration to protein folding thermodynamics. 2. The entropy and Gibbs energy of hydration. *J. Mol. Biol.* **232**, 660–679.
10. Makhatadze, G. I. & Privalov, P. L. (1993). Contribution of hydration to protein folding thermodynamics. 1. The enthalpy of hydration. *J. Mol. Biol.* **232**, 639–659.
11. Yang, A.-S., Sharp, K. A. & Honig, B. (1992). Analysis of the heat capacity dependence of protein folding. *J. Mol. Biol.* **227**, 889–900.

12. Jackson, M. B. & Sturtevant, J. M. (1978). Phase transitions of the purple membranes of *Halobacterium halobium*. *Biochemistry*, **17**, 911–915.
13. Heyes, C. D. & El Sayed, M. A. (2001). Effect of temperature, pH, and metal ion binding on the secondary structure of bacteriorhodopsin: FT-IR study of the melting and premelting transition temperatures. *Biochemistry*, **40**, 11819–11827.
14. Heyes, C. D. & El Sayed, M. A. (2002). The role of the native lipids and lattice structure in bacteriorhodopsin protein conformation and stability as studied by temperature-dependent Fourier transform-infrared spectroscopy. *J. Biol. Chem.* **277**, 29437–29443.
15. Echabe, I., Haltia, T., Freire, E., Goni, F. M. & Arrondo, J. L. (1995). Subunit III of cytochrome c oxidase influences the conformation of subunits I and II: an infrared study. *Biochemistry*, **34**, 13565–13569.
16. Morin, P. E. & Freire, E. (1991). Direct calorimetric analysis of the enzymatic activity of yeast cytochrome c oxidase. *Biochemistry*, **30**, 8494–8500.
17. Morin, P. E., Diggs, D. & Freire, E. (1990). Thermal stability of membrane-reconstituted yeast cytochrome c oxidase. *Biochemistry*, **29**, 781–788.
18. Landin, J. S., Katragadda, M. & Albert, A. D. (2001). Thermal destabilization of rhodopsin and opsin by proteolytic cleavage in bovine rod outer segment disk membranes. *Biochemistry*, **40**, 11176–11183.
19. Epanand, R. F., Epanand, R. M. & Jung, C. Y. (2001). Ligand-modulation of the stability of the glucose transporter GLUT 1. *Protein Sci.* **10**, 1363–1369.
20. Lepock, J. R., Rodahl, A. M., Zhang, C., Heynen, M. L., Waters, B. & Cheng, K. H. (1990). Thermal denaturation of the Ca<sup>2+</sup>(+)-ATPase of sarcoplasmic reticulum reveals two thermodynamically independent domains. *Biochemistry*, **29**, 681–689.
21. Arkin, I. T., Sukharev, S. I., Blount, P., Kung, C. & Brünger, A. T. (1998). Helicity, membrane incorporation, orientation and thermal stability of the large conductance mechanosensitive ion channel from *E. coli*. *Biochim. Biophys. Acta*, **1369**, 131–140.
22. Creighton, T. E. (1992). *Protein Folding*. W. H. Freeman and Company, New York.
23. Bishop, C. M., Walkenhorst, W. F. & Wimley, W. C. (2001). Folding of  $\beta$ -sheet membrane proteins: specificity and promiscuity in peptide model systems. *J. Mol. Biol.* **309**, 975–988.
24. Wimley, W. C., Hristova, K., Ladokhin, A. S., Silvestro, L., Axelsen, P. H. & White, S. H. (1998). Folding of  $\beta$ -sheet membrane proteins: a hydrophobic hexapeptide model. *J. Mol. Biol.* **277**, 1091–1110.
25. Ladokhin, A. S. & White, S. H. (1999). Folding of amphipathic  $\alpha$ -helices on membranes: energetics of helix formation by melittin. *J. Mol. Biol.* **285**, 1363–1369.
26. Wieprecht, T., Apostolov, O., Beyermann, M. & Seelig, J. (1999). Thermodynamics of the alpha-helix-coil transition of amphipathic peptides in a membrane environment: implications for the peptide-membrane binding equilibrium. *J. Mol. Biol.* **294**, 785–794.
27. Wenk, M. R. & Seelig, J. (1998). Magainin 2 amide interaction with lipid membranes: calorimetric detection of peptide binding and pore formation. *Biochemistry*, **37**, 3909–3916.
28. White, S. H., Wimley, W. C., Ladokhin, A. S. & Hristova, K. (1998). Protein folding in membranes: determining the energetics of peptide-bilayer interactions. *Methods Enzymol.* **295**, 62–87.
29. Wimley, W. C. & White, S. H. (1993). Membrane partitioning: distinguishing bilayer effects from the hydrophobic effect. *Biochemistry*, **32**, 6307–6312.
30. Li, Y., Han, X. & Tamm, L. K. (2003). Thermodynamics of fusion peptide-membrane interactions. *Biochemistry*, **42**, 7245–7251.
31. Schulz, G. E. (2000).  $\beta$ -Barrel membrane proteins. *Curr. Opin. Struct. Biol.* **10**, 443–447.
32. Deisenhofer, J., Epp, O., Miki, K., Huber, R. & Michel, H. (1984). X-ray structure analysis of a membrane protein complex: electron density map at 3 Å resolution and a model of the chromophores of the photosynthetic reaction center from *Rhodospseudomonas viridis*. *J. Mol. Biol.* **180**, 385–398.
33. Wimley, W. C. & White, S. H. (1996). Experimentally determined hydrophobicity scale for proteins at membrane interfaces. *Nature Struct. Biol.* **3**, 842–848.
34. Selsted, M. E., Novotny, M. J., Morris, W. L., Tang, Y.-Q., Smith, W. & Cullor, J. S. (1992). Indolicidin, a novel bactericidal tridecapeptide amide from neutrophils. *J. Biol. Chem.* **267**, 4292–4295.
35. Yau, W. M., Wimley, W. C., Gawrisch, K. & White, S. H. (1998). The preference of tryptophan for membrane interfaces. *Biochemistry*, **37**, 14713–14718.
36. White, S. H. & Wimley, W. C. (1998). Hydrophobic interactions of peptides with membrane interfaces. *Biochim. Biophys. Acta*, **1376**, 339–352.
37. Marsh, D. (1990). *CRC Handbook of Lipid Bilayers*. CRC Press, Boca Raton.
38. Makhatadze, G. I., Lopez, M. M. & Privalov, P. L. (1997). Heat capacities of protein functional groups. *Biophys. Chem.* **64**, 93–101.
39. Terzi, E., Hölzemann, G. & Seelig, J. (1994). Reversible random coil- $\beta$ -sheet transition of the Alzheimer  $\beta$ -amyloid fragment. *Biochemistry*, **33**, 1345–1350.
40. Scholtz, J. M., Marqusee, S., Baldwin, R. L., York, E. J., Stewart, J. M., Santoro, M. & Bolen, D. W. (1991). Calorimetric determination of the enthalpy change for the  $\beta$ -helix to coil transition of an alanine peptide in water. *Proc. Natl Acad. Sci. USA*, **88**, 2854–2858.
41. Wimley, W. C., Hristova, K., Ladokhin, A. S., Silvestro, L., Axelsen, P. H. & White, S. H. (1998). Folding of  $\beta$ -sheet membrane proteins: a hydrophobic hexapeptide model. *J. Mol. Biol.* **277**, 1091–1110.
42. Bishop, C. M., Walkenhorst, W. F. & Wimley, W. C. (2001). Folding of  $\beta$ -sheet membrane proteins: specificity and promiscuity in peptide model systems. *J. Mol. Biol.* **309**, 975–988.
43. White, S. H. & Wimley, W. C. (1999). Membrane protein folding and stability: physical principles. *Annu. Rev. Biophys. Biomol. Struct.* **28**, 319–365.
44. Yau, W. M., Wimley, W. C., Gawrisch, K. & White, S. H. (1998). The preference of tryptophan for membrane interfaces. *Biochemistry*, **37**, 14713–14718.
45. Wimley, W. C. (2002). Toward genomic identification of beta-barrel membrane proteins: composition and architecture of known structures. *Protein Sci.* **11**, 301–312.
46. Wiener, M. C. & White, S. H. (1992). Structure of a fluid dioleoylphosphatidylcholine bilayer determined by joint refinement of X-ray and neutron diffraction data. III. Complete structure. *Biophys. J.* **61**, 434–447.
47. Doyle, D. A. & Wallace, B. A. (1997). Crystal structure of the gramicidin/potassium thiocyanate complex. *J. Mol. Biol.* **266**, 963–977.
48. Ketchum, R. R., Roux, B. & Cross, T. A. (1997). High-resolution polypeptide structure in a

- lamellar phase lipid environment from solid state NMR derived orientational constraints. *Structure*, **5**, 1655–1669.
49. Mayer, L. D., Hope, M. J. & Cullis, P. R. (1986). Vesicles of variable sizes produced by a rapid extrusion procedure. *Biochim. Biophys. Acta*, **858**, 161–168.
50. Wimley, W. C. & White, S. H. (1993). Quantitation of electrostatic and hydrophobic membrane interactions by equilibrium dialysis and reverse-phase HPLC. *Anal. Biochem.* **213**, 213–217.

*Edited by I. B. Holland*

*(Received 7 April 2004; received in revised form 21 June 2004; accepted 23 June 2004)*